Title: The ability to cross the blood-cerebrospinal fluid barrier is a generic property of acute lymphoblastic leukaemia blasts.

Running title: CNS infiltration in BCP-ALL

Authors: Mark TS Williams[1*], Yasar M Yousafzai[1,2*], Alex Elder[3*], Klaus Rehe[3,8], Simon Bomken[3,8], Liron Frishman-Levy[4,5], Sigal Tavor[6], Paul Sinclair[3], Katie Dormon[3], Dino Masic[3] , Tracey Perry[7], Victoria J Weston[7], Pamela Kearns[7], Helen Blair[3], Lisa J Russell[3], Olaf Heidenreich[3], Julie AE Irving[3], Shai Izraeli[4,5],Josef Vormoor[3, 8], Gerard J Graham[1], Christina Halsey[9,10].

[1] Centre for Immunobiology, Institute of Infection, Immunity and Inflammation, College of Medical, Veterinary and Life Sciences, University of Glasgow, UK.

[2] Institute of Basic Medical Sciences, Khyber Medical University, Peshawar, Pakistan.

[3] Northern Institute for Cancer Research, Newcastle University, UK.

[4] Functional Genomics and Childhood Leukemia Research Center, Sheba Medical Center, Tel-Hashomer, Ramat Gan, Israel

[5] Department of Human Molecular Genetics and Biochemistry, Sackler Medical School, Tel Aviv University, Tel Aviv, Israel

[6] Goldyne Savad Institute of Gene Therapy, Hadassah Hebrew University Hospital, Jerusalem, Israel.

[7] Institute of Cancer and Genomic Sciences, University of Birmingham, UK.

[8] Department of Paediatric and Adolescent Haematology and Oncology, Great North Children's Hospital, Newcastle upon Tyne Hospitals NHS Foundation Trust, Newcastle upon Tyne, UK.

[9] Wolfson Wohl Cancer Research Centre, Institute of Cancer Sciences, College of Medical, Veterinary and Life Sciences, University of Glasgow, UK

[10] Department of Paediatric Haematology, Royal Hospital for Children, Glasgow, UK.

* These three authors contributed equally to this work

Corresponding author: Dr Christina Halsey, Institute of Cancer Sciences, College of Medical, Veterinary and Life Sciences, University of Glasgow, Glasgow G61 1QH, UK. Email: chris.halsey@glasgow.ac.uk, telephone +44 141 3308135, Fax +44 141 3304297.

Financial Support: This work was supported by the Kay Kendall Leukaemia Fund (KKL454, KKL515) (CH, LR) with additional funding from Cancer Research UK (C27943/A12788) (JV, OH), Leukaemia & Lymphoma Research (DM, TP, KD, PK), the European Research Council (PS), the WLBH Foundation & Chief Scientist Health Ministry ERA-NET grant (SI), the Chief Scientists' Office (SCD/08) (CH), the Scottish Funding Council (CH) a Wellcome Trust Senior Investigator award (GG) and the Medical Research Council (G0901113, G0802259) (GG, SB).

ABSTRACT

Prevention of central nervous system (CNS) relapse is critical for cure of childhood B-cell precursor acute lymphoblastic leukaemia (BCP-ALL). Despite this, mechanisms of CNS infiltration are poorly understood and the timing, frequency and properties of BCP-ALL blasts entering the CNS compartment are unknown. We investigated the CNS-engrafting potential of BCP-ALL cells xenotransplanted into immunodeficient NOD.Cg-*Prkdc*^{scid}*Il2rg*^{tm1Wjl}/SzJ mice. CNS engraftment was seen in 23/29 diagnostic samples (79%), 2/2 from patients with overt CNS disease and 21/27 (78%) from patients thought to be CNS-negative by diagnostic lumbar puncture. Histological findings mimic human pathology and demonstrate that leukaemic cells primarily transit the blood-cerebrospinal-fluid barrier sitting in close proximity to the dural sinuses – the site of recently discovered CNS lymphatics. Retrieval of blasts from the CNS showed no evidence for chemokine receptor-mediated selective trafficking. The high frequency of infiltration and lack of selective trafficking led us to postulate that CNS tropism is a generic property of leukaemic cells. To test this we performed serial dilution experiments, CNS engraftment was seen in 5/6 mice following transplantation of as few as 10 leukaemic cells. Finally, clonal tracking techniques confirmed the polyclonal nature of CNS infiltrating cells with multiple clones engrafting in both the CNS and periphery. Overall, these findings suggest that sub-clinical seeding of the CNS is likely to be present in the majority of BCP-ALL patients at original diagnosis and efforts to prevent CNS relapse should concentrate on augmenting effective eradication of disease from this site, rather than targeting entry mechanisms.

INTRODUCTION

One of the earliest advances in curative treatment for childhood acute lymphoblastic leukaemia (ALL) came with the recognition that without central nervous system (CNS) directed therapy up to 75% of children relapse within the CNS [1]. Introduction of universal CNS-directed treatment resulted in a dramatic reduction in overt CNS relapses. However, disease in the CNS still poses many clinical challenges [2]. CNS-directed therapy is potentially toxic to the developing brain [3] and efforts to risk-stratify and devise less toxic therapy are hampered by a lack of knowledge regarding mechanisms of CNS disease and the absence of biomarkers predictive of CNS relapse.

CNS involvement is classified by identification of lymphoblasts in cytospin preparations of cerebrospinal fluid (CSF); CNS-1 (CSF white cell count (WCC) <5/µl, no blasts), CNS-2 (WCC<5/µl, visible blasts) or CNS-3 (WCC>5/µl). It is important to appreciate that CNS-1 status does not equate with absence of leukaemia in the central nervous system, early post-mortem studies on children succumbing to leukaemia frequently showed leptomeningeal involvement despite negative CSF cytology [4]. Cytological classification is insensitive [5-7] and clearly inadequate for risk stratification since the majority of relapses occur in CNS-1 children [8,9] In addition, the CNS is one of the major sites of relapse in children with otherwise excellent prognosis as determined by low-risk bone marrow (BM) minimal residual disease measurements [10] suggesting that factors influencing leukaemic kill in the periphery may not apply to the CNS. It is clear that a better understanding of CNS disease is required in order to develop rational risk-stratified treatment.

Two possible models for CNS relapse can be postulated (see Figure 1). Firstly, it is possible that only some leukaemic cells acquire the ability to enter the CNS and the risk

of CNS relapse depends on the presence or absence of a clone with the capacity to leave the bone marrow and enter the CNS – this may occur at diagnosis or later during the disease course (model 1). Alternatively, all leukaemic cells may have the ability to seed this compartment and sub-clinical CNS involvement at diagnosis may be universal. In this case CNS relapse is determined by whether cells can adapt to the foreign microenvironment of the CNS and evade elimination by ALL-directed therapy and/or immunological surveillance (model 2). Distinguishing between these two models is critical in order to determine the optimal approaches for risk stratification, development of biomarkers and novel therapeutics to prevent CNS relapse.

Here we describe experiments that test these alternative models by addressing the qualitative question of whether every leukaemic blast and/or every individual patient/subtype of leukaemia has the intrinsic capacity to enter the CNS. We demonstrate that primary BCP-ALL blasts, even from low risk CNS-1 patients, frequently infiltrate the CNS in xenograft models by transiting the Blood-CSF barrier. We find no evidence for selective trafficking of subclones to the CNS but rather show that CNS infiltration is a generic and ubiquitous property of BCP-ALL cells. These findings support the current dogma that all children require CNS-directed therapy and suggest that novel therapies to reduce the risk of CNS relapse and/or to provide safer and less toxic CNS directed therapy should concentrate on effective eradication of cells from this site rather than targeting selected entry mechanisms.

MATERIALS AND METHODS

Cell culture and primary cells

SD1, REH (DSMZ, Braunschweig, Germany) and Sup B15 (ATCC, LGC-standards Middlesex, UK) cell lines were grown at 37^{o}C, 5% CO_2 in complete RPMI 1640, 10% fetal bovine serum (FBS), 1% Penicillin/Streptomycin (Invitrogen, Paisley UK). Human primary meningeal cells (Cat #1400) and choroid-plexus epithelial cells (Cat #1310) were obtained from ScienCell laboratories (Carlsbad, CA, USA) and cultured according to supplier's instructions.

Following informed consent, diagnostic bone marrow samples from children with BCP-ALL underwent mononuclear cell enrichment using density-gradient centrifugation (Ficoll-Paque; GE Healthcare, Amersham, UK), cryopreservation in 10% DMSO/90%FBS and storage in liquid nitrogen until use. Samples originated from local institutions and the Leukaemia & Lymphoma Research (LLR) Childhood Leukaemia Cell Bank. Table 1 and supplementary table 1 list patient details. Use of human samples was approved by the West of Scotland Research Ethics Committee. ScienCell primary tissues are obtained following informed consent (www.sciencellonline.com/site /ethics.php).

Xenotransplants

JAX® NOD.Cg-*Prkdc*^{scid}*Il2rg*^{tm1Wjl}/SzJ (NSG) (Charles River, Europe), or NOD.Cg-*Prkdc*^{scid}*IL2rg*^{tm1Sug}/JicTac (CIEA NOG®) (Taconic, Ry, Denmark) mice were kept in sterile isolators with autoclaved food, bedding and water. Xenotransplantation was performed at 6-10 weeks of age using intravenous (tail vein) or intrafemoral injections of up to 1x10^{7} leukaemic cells, as previously described [11]. Supplementary tables 2 and 3 give details of individual experiments. Methods for serial dilution and sorting of leukaemic subpopulations have been published [11]. Mice were humanely killed once they became unwell, had clinical evidence of leukaemia or significant weight loss. All

animal experiments were approved by Institutional Ethical Review Process Committees and performed under UK Home Office licences.

Histology

Murine heads were stripped of soft tissues, fixed in 10% Neutral Buffered Formalin (NBF) (CellPath, Powys, UK) and decalcified in Hilleman and Lee EDTA solution (5.5% EDTA in 10% formalin) for 2-3 weeks. Samples were processed as described previously [12].

Anti-CD45 immunohistochemistry on paraffin-embedded sections was performed as previously described [13].

Imaging used Axiostar-plus or AxioImager-M2 microscopes with Axiovision and Zen software (Carl Zeiss, Cambridge, UK).

Cell retrieval

Following terminal CO_2 asphyxiation mice were perfused with phosphate-buffered saline (PBS) to eliminate peripheral blood contamination. Pilot experiments were performed comparing retrieval of leukaemic cells from the meninges alone vs. performing whole brain extracts of meninges and parenchyma. The former produced excellent yields of pure leukaemic cells, whilst the latter did not add to the yield and substantially reduced the viability and purity of the retrieved cells. Therefore, all experiments utilised direct retrieval of leukaemic cells from the leptomeninges by gentle scraping of the skull vault and vortexing the whole brain in PBS for 5 minutes. Femoral BM cells were retrieved by flushing with PBS. Spleen samples were collected by homogenising material through a cell strainer with PBS.

Quantitative PCR

RNA extraction, on-column DNase digestion, cDNA synthesis and custom designed Taqman low density arrays (TLDA) were performed as described previously [14]. Two

reference endogenous control genes were included on the plate; TATA binding protein (TBP) and 18sRNA. Gene Assay IDs are given in supplementary data table 4. Both reference genes were validated according to MIQE guidelines[15]. Data were analysed using the ΔΔCT method using RQ Manager 1.2.4 software (Applied Biosystems, Paisley, UK). For gene expression arrays, arbitrary expression values were derived from the CT value as described previously [16]. Gene expression assay IDs are given in Supplementary Table 4.

Flow cytometry

Cells were washed twice in PEF (0.5% FCS, 0.5mM EDTA in PBS), incubated with anti-human Fc-receptor binding inhibitor (eBioscience, Hatfield, UK) and then with directly conjugated antibodies (supplementary table 5). Viability staining used Viaprobe (BD Biosciences, Oxford, UK), or DRAQ7 (Biostatus, Shepshed, UK). Data were acquired on a MACSQuant flow cytometer (Miltenyi Biotec) and analysed using FlowJo 7.2.4 software (Tree Star Inc, Ashland, OR USA).

Clonal tracking

Primograft ALL blasts were lentivirally transduced and transplanted intrafemorally into NSG mice as described previously [17]. Genomic DNA was extracted from splenic and leptomeningeal leukaemic blasts using a DNeasy kit (Qiagen). Analysis of lentiviral integration sites using non-restriction-based linear amplification mediated PCR (nrLAM-PCR) was described previously [18]. The linear PCR step was performed using a biotinylated primer (Btn-GCACTGACAATTCCGTGGTGTT GTC) for 99 cycles (98 °C for 10 s, 64 °C for 45 s and 72 °C for 15 s). The final amplification used two successive 30 cycle PCR reactions (98 °C for 10 s, 62 °C for 30 s and 72 °C for 2 min) with the following primers: Round 1 Fw GACCCGGGAGATCTGAATTC, Rev GCTACGTAACTCCCAACGAAG; Round 2: Fw AGTGGCACAGCAGTTAGG, Rev

GTGTGGAAAATCTCTAGCA). Illumina adaptors were added by PCR and samples were sequenced using an Illumina MiSeq. Reads were considered valid if they perfectly matched the expected vector flanking sequence. Sequences comprising less than 0.1% of the total were removed, and reads with truncations or mismatches within the remaining sequences were merged to create the final list.

Statistics

Student's t-tests were used to analyse 2 parametric groups and Chi-squared tests were used to examine frequency of CNS infiltration. A p-value of ≤ 0.05 was considered significant. All analyses were performed using GraphPad Prism (La Jolla, CA, USA).

RESULTS

CNS engraftment in NSG mice is common and involves passage across the blood-CSF barrier

To investigate the frequency and distribution of CNS engraftment, brains were examined from NSG mice xenografted with 29 different ALL samples (diagnostic BM samples and primary cells previously passaged through mice (primografts), see supplementary tables 1-3 for clinical and experimental details). CNS engraftment was observed in 23/29 patient samples (79%) across 13 different cytogenetic subtypes (Table 1). There was no difference in the frequency of CNS engraftment in primary BM samples vs. primografts ($p= 0.303$, Chi-squared test). CNS engraftment was seen in samples with both high and low risk clinical features (Table 2) and semi-quantitative scoring of the degree of CNS infiltration did not show clear differences between high and low risk samples (supplementary data table 2). Histopathology was consistent; showing early infiltration around the dural venous sinuses, plaques of disease in the

leptomeninges, relative sparing of the ventricles and absence of gross parenchymal involvement (Figure 2a-c). This indicates that ALL cells primarily transit the blood-CSF barrier (comprising the choroid plexus and the meningeal post-capillary venules) rather than the blood-brain barrier. Importantly, this histopathology closely resembles that observed in patients (Figure 2d) [4,19].

Our original panel of primografts and primary samples mainly comprised CNS-1 patients (table 1). Therefore, CNS-engrafting capacity appears to be more prevalent than suggested by CSF-cytospin status. However, since primograft samples have, *a priori*, shown successful engraftment in mice, there may have been a selection bias for aggressive leukaemias. To address this, we prospectively investigated CNS engraftment of BM-derived leukaemic cells from a CNS-3 patient (#5094) and 5 matched CNS-1 controls (#4736, #5449, #6112, #5705 and #4630). These samples had unknown xenografting capability and all carried the good-prognosis translocation *t(12;21)*. All samples engrafted in the BM whilst CNS infiltration was seen in the CNS-3 sample but also in 4/5 CNS-1 samples (Figure 2e).

Together these observations indicate that the majority of diagnostic BCP-ALL BM samples contain cells capable of entering the CNS compartment, irrespective of initial CSF cytospin findings.

Chemokine receptors do not drive CNS entry in BCP-ALL.

In a murine model of T-ALL, expression of the chemokine receptor CCR7 determines CNS engraftment [20]. In addition, a recent report has highlighted a possible association between CXCR3 expression and ALL migration to the CNS [21]. Therefore, we investigated the role of chemokine receptors in directing leukaemic cells to the CNS compartment in our model. As shown in Figure 3 and Supplementary Figure 1 and 2

only CXCR3 and CXCR4 were consistently expressed on the cell surface with variable expression of CCR7 and CCR6 (figure 3a) and CXCR7 (supplementary figure 2). Comparison of chemokine receptor expression in two non-CNS homing primary samples (#4630 and #5969) showed the same pattern of chemokine receptor expression as 7 CNS homing primary samples (Figure 3a and Supplementary Table 6). Therefore, there was no apparent chemokine receptor expression signature that marked the ability to enter the CNS compartment. Next, we examined the repertoire of chemokine ligands expressed by human blood-CSF barrier tissues. Importantly, the CXCR3 ligand CXCL10, the CXCR4/CXCR7 ligand CXCL12 and the CCR6 ligand CCL20 were detected (Figure 3b), suggesting these pairings could be functionally important in ALL transit across this barrier. To investigate whether cells expressing high levels of any particular chemokine receptor were being positively selected for in the CNS compartment *in vivo* we compared expression profiles of leukaemic cells retrieved from the meninges and BM of engrafted mice. As seen in Figure 3c there was no evidence of positive selection for high-expressing sub-clones in the CNS, with leukaemic blasts showing similar chemokine receptor expression profiles at the two sites. Finally, given the importance of the chemokine receptor CXCR4 in BM engraftment, we went on to specifically interrogate the role of CXCR4 in CNS engraftment by utilising the CXCR4 inhibitor AMD3100 *in vivo*. Interestingly, mice in the AMD3100 treated group showed a significant reduction in leukaemic burden in the liver and BM, but no reduction of CNS disease (Fig 3d and Supplementary Figure 3).

Therefore, although chemokine receptors may play a permissive role in ALL transit across the blood-CSF barrier, single members do not appear to play an instructive role in determining localisation of leukaemic blasts in the CNS compartment.

CNS leukaemia initiating cells are frequent and not related to blast maturation status.

Overall, the evidence of frequent CNS involvement and lack of chemokine receptor mediated selective trafficking to the CNS suggested to us that CNS-engrafting capability may be a generic property of BCP-ALL lymphoblasts rather than an acquired property of a rare sub-clone. To test this, we examined the frequency of cells within an individual leukaemia sample capable of CNS engraftment. Using a cohort of *BCR-ABL* and *BCR-ABL*-like (defined as an activated kinase gene expression profile which clusters with *BCR-ABL* on microarray but without a classical Philadelphia chromosome [22]) samples, cell suspensions were prepared containing 10, 100, 1000 or 1500 cells for intrafemoral transplantation (Figure 4a). The results of BM engraftment in this cohort of mice are already published [11]. Figure 4a shows no relationship between cell number and likelihood of CNS engraftment and as few as 10 cells produced CNS disease in 5/6 cases (Figure 4a and Supplementary Table 3).

Since the ability to egress from the BM to the periphery is acquired during normal B-cell development we next investigated whether CNS engraftment rates differed in mature *vs*. immature ALL subpopulations. Leukaemia propagating ability in childhood ALL does not appear to follow a hierarchical stem cell model [11,23] and indeed a stem cell-like transcriptional signature is seen in both CD34+ and CD34- ALL blasts [11]. However, down-regulation of CD34 expression in ALL is associated with increased expression of B-cell differentiation genes [23] and diagnostic BCP-ALL samples contain blasts at different maturation stages [11]. B-cell precursors were identified by gating on CD19 and then flow-sorted into $CD34^{high}$ (immature), $CD34^{low}$ (more mature), $CD10^{low}$ (immature), $CD10^{high}$ (more mature) and $CD20^{low}$ (immature), $CD20^{high}$ (more mature) populations. Sorted cells underwent limiting dilution and 10-1500 cells were injected intrafemorally (Supplementary Table 3). As seen in Figure 4b all fractions showed

CNS-engrafting capability and both immature and more mature B-cell subpopulations appeared to engraft in the CNS with equal competence.

These experiments support our hypothesis that the ability to enter the CNS is not restricted to rare subclones but is instead a generic property of the majority of leukaemic cells present at original diagnosis.

Clonal tracking experiments identify very similar clonal composition in CNS and periphery

To lend further support to our hypothesis we performed clonal tracking of lentivirally marked #WB51 primograft cells, which carry the Philadelphia chromosome, and #L707 cells which have a t(17;19) translocation. This allowed us to investigate both the clonal architecture of leukaemic subpopulations in the CNS and their relationship to cells in the periphery. This was achieved using a modified linear amplification-mediated PCR (LAM-PCR) protocol [18] to detect lentiviral integration sites in samples from the spleen and leptomeninges. Each integration site is unique, so can be used as a heritable marker to track the spread of individual clones (Figure 5a). Up to 10,000 cells were transplanted per mouse, with a maximum lentiviral transduction rate of 10% to limit the risk of multiple integrations in a single cell [24]. Analysis of the most prevalent integrations in two mice per sample demonstrated that the CNS disease was polyclonal and very similar in clonal composition to the splenic disease (Figure 5b and Supplementary Figure 5). All integrations present in the spleen at >0.5% of the total population were also detectable in the meninges, demonstrating that all major clones had CNS engrafting capability. In the case of #WB51 femoral leukaemic cells were also analysed and again all detectable clones in the femur were also present in the CNS (supplementary figure 5).

Together these experiments confirm our hypothesis that the ability to engraft in the CNS is a generic property of the bulk leukaemic population at initial diagnosis, rather than being due to acquisition of a metastatic phenotype by a rare sub-clone.

DISCUSSION

We have shown that CNS involvement is detectable in more than three-quarters of xenografts from diagnostic primary BCP-ALL samples and is seen with equal frequency in samples from patients with high- and low-risk cytogenetic and clinical features. These observations support a model whereby CNS relapse is determined by whether cells can adapt to the foreign microenvironment of the CNS and evade elimination by ALL-directed therapy and/or immunological surveillance (model 2), rather than whether individual clones present within a patients leukaemia acquire the ability to enter the CNS compartment (model 1) (illustrated in figure 1). The importance of this observation lies in the concept that CNS infiltration is likely to be present in the majority of patients at the time of diagnosis. Current cytological classification may lead to the erroneous impression that CNS-1 patients do not have any leukaemia in the CNS, and consequently that these children are at very low risk of CNS relapse..

We acknowledge some limitations in the clinical interpretation of our work. Xenograft models are unlikely to completely faithfully recapitulate all the receptor-ligand interactions governing leukaemic engraftment in humans, although most trafficking molecules are highly conserved [25] and this limitation would be predicted to result in reduced rather than enhanced engraftment in xenografts. In addition, our limiting dilution and clonal tracking experiments were performed using high risk leukaemias which may more readily engraft in mice[26-28]. However, our original cohort of mice

showed frequent CNS involvement in both high and low-risk primary samples suggesting this is a universal property of BCP-ALL cells. Additional support for high rates of sub-clinical seeding of the CNS at the time of diagnosis comes from clinical observations. The use of more sensitive detection methods such as flow cytometry [7] and PCR [5,6] are able to detect occult CNS involvement in up to 40% of patients. In addition, prior to the era of routine CNS "prophylaxis", 50-75% of children relapsed the CNS [1], usually within a couple of months of original diagnosis, suggesting occult CNS leukaemia was present from the outset. This rate of early CNS relapse in patients mirrors the rate of CNS infiltration in our xenograft model.

Post-mortem histopathology from children with ALL demonstrates a pattern of CNS infiltration closely resembling our xenograft model [4]. The earliest leukaemic infiltrates appear in the walls of superficial arachnoid veins, with progressive infiltration of the leptomeninges and subsequent extension into the deep arachnoid following the course of penetrating vessels. Parenchymal infiltration is only seen in late stage disease, always accompanied by a breach of the pia-glial membrane [4]. Therefore our results, along with these historical data, provide evidence for ALL cells primarily transiting the blood-CSF barrier rather than the blood-brain barrier. This is important when considering cellular trafficking, microenvironmental influences and drug pharmacokinetics as the leptomeninges and brain parenchyma are distinct physiological compartments [29]. In addition, it highlights that commonly used *in vitro* models of the blood brain barrier are inappropriate to study mechanisms of CNS entry of leukaemic blasts. The close relationship of leukaemic cells to the dural sinuses is particularly intriguing given the recent description of lymphatic vessels in this area in mice [30]. Of note, our histology and the human post-mortem data [4] also show ALL blasts adherent to meningeal stroma rather than free-floating in the CSF. This may explain why

sampling a small volume of CSF from the lumbar-spine may significantly underestimate CNS infiltration.

We went on to examine whether chemokine receptors directed this migration across the blood-CSF barrier. In common with previous reports[21,31-33] we show that BCP-ALL cells express CXCR3 and CXCR4 with some samples expressing CCR7, CCR6 and CXCR7. Corresponding chemokine ligands were expressed by blood-CSF barrier tissues. However, there was no evidence for positive selection of cells bearing these receptors within the CNS compartment. Previous work has shown that CXCR3 inhibitors cause a global reduction in leukaemic engraftment in BM, spleen and CNS[21]. In contrast, we have shown that treatment with the CXCR4 inhibitor AMD3100 leads to a reduced disease burden in the liver and BM but no reduction in CNS infiltration suggesting CNS engraftment may be a CXCR4 independent niche.

Our findings differ from results in T-ALL, where a single chemokine receptor ligand pairing (CCR7-CCL19) determined the ability of lymphoblasts to enter the CNS in a humanised murine model [20]. Our findings may be due to differences in experimental models[34], or the intrinsic biology of T- and B-cells; CCR7 expressing memory T-cells are the most abundant leukocyte to be found in normal CSF [35] and so it is perhaps not surprising that CCR7 expression enhances T-ALL entry into this site.

Lastly, we investigated the subclonal composition of the CNS compartment. We found that CNS engrafting ability was a generic ability of leukaemic cells and that the clonal composition of CNS and splenic engrafting cells was remarkably similar. This suggests that CNS infiltrating ability is ubiquitous in BCP-ALL and strongly argues against our proposed model 1 and supports model 2 i.e. that CNS relapse originates from inadequate eradication of cells from this sanctuary site rather than selective entry (Figure 1).

Of note our studies do not exclude that individual cells/clones differ in their biological fitness to invade, proliferate and survive in the CNS but do indicate that CNS invasion is a generic ability of the leukaemic blasts. Differences in biological fitness may determine leukaemic load in the CNS and thus explain why some children have visible disease on CSF cytology and others do not, and may play a role in the likelihood of survival of cells in this compartment and the attendant risk of CNS relapse. Future efforts to investigate risk factors for CNS relapse should focus on advantageous leukaemic adaptations to this new niche, using approaches such as transcriptomics, metabolomics and proteomics. We and others have reported on the potential role of the cytokine interleukin-15 in promoting leukaemic cell survival in the hostile environment in the CSF [13,36]. A recent report has highlighted a critical role for MER tyrosine kinase in promoting survival of t(1:19) positive ALL in the CNS[37] and increased ICAM-1[38], SCD and Osteopontin[39] expression have also been associated with CNS disease . Additional mechanisms of CNS relapse may relate to evasion of chemotherapy [40] or immune surveillance [34,41] at this site.

Finally, our findings have important implications for the design of risk-adapted CNS therapy. Firstly, our studies indicate that the current dogma of CNS-directed therapy for all patients appears to have a rational scientific basis. Secondly, it is unlikely that chemokine receptor expression profiling will be a useful biomarker for CNS disease in BCP-ALL. Thirdly, identifying factors that enable long-term survival of cells in the CNS (which may also enhance long-term survival in the bone marrow) may be a better therapeutic strategy than attempts to block cell entry.

Acknowledgements

We gratefully acknowledge the LLR Childhood Leukaemia Cell Bank, the ALL2003 trial co-ordinators, CTSU Oxford, and all contributing centres and patients. We thank Lynn Stevenson, Alasdair Fraser and Michelle Le Brocq (University of Glasgow) for technical assistance and Monique den Boer (Rotterdam) for the original bcr-abl like samples.

Authorship

CH, JV, OH, SI and GG designed the research, analysed data and wrote the paper. YY, MW and AE performed the experiments, analysed the data and contributed to writing the paper. KR, ST, LFL and SB performed the experiments. PS, KD, DM, TP, VW, PK, HB, LJR, and JAEI performed the xenografting experiments and provided essential data. All authors contributed to the writing of the manuscript.

Conflicts of Interest

All authors have no conflict of interest to declare.

REFERENCES

1. Evans AE, Gilbert ES, Zandstra R. The increasing incidence of central nervous system leukemia in children. (Children's Cancer Study Group A). *Cancer*. 1970;26(2):404-409.
2. Pui CH, Howard SC. Current management and challenges of malignant disease in the CNS in paediatric leukaemia. *Lancet Oncol*. 2008;9(3):257-268.
3. Halsey C, Buck G, Richards S, Vargha-Khadem F, Hill F, Gibson B. The impact of therapy for childhood acute lymphoblastic leukaemia on intelligence quotients; results of the risk-stratified randomized central nervous system treatment trial MRC UKALL XI. *J Hematol Oncol*. 2011;4:42.
4. Price RA, Johnson WW. The central nervous system in childhood leukemia. I. The arachnoid. *Cancer*. 1973;31(3):520-533.

5. Pine SR, Yin C, Matloub YH, et al. Detection of central nervous system leukemia in children with acute lymphoblastic leukemia by real-time polymerase chain reaction. *J Mol Diagn*. 2005;7(1):127-132.
6. Scrideli CA, Queiroz RP, Takayanagui OM, Bernardes JE, Melo EV, Tone LG. Molecular diagnosis of leukemic cerebrospinal fluid cells in children with newly diagnosed acute lymphoblastic leukemia. *Haematologica*. 2004;89(8):1013-1015.
7. Martinez-Laperche C, Gomez-Garcia AM, Lassaletta A, et al. Detection of occult cerebrospinal fluid involvement during maintenance therapy identifies a group of children with acute lymphoblastic leukemia at high risk for relapse. *Am J Hematol*. 2013;88(5):359-364.
8. Krishnan S, Wade R, Moorman AV, et al. Temporal changes in the incidence and pattern of central nervous system relapses in children with acute lymphoblastic leukaemia treated on four consecutive Medical Research Council trials, 1985-2001. *Leukemia*. 2010;24(2):450-459.
9. Burger B, Zimmermann M, Mann G, et al. Diagnostic cerebrospinal fluid examination in children with acute lymphoblastic leukemia: significance of low leukocyte counts with blasts or traumatic lumbar puncture. *J Clin Oncol*. 2003;21(2):184-188.
10. Vora A, Goulden N, Wade R, et al. Treatment reduction for children and young adults with low-risk acute lymphoblastic leukaemia defined by minimal residual disease (UKALL 2003): a randomised controlled trial. *Lancet Oncol*. 2013;14(3):199-209.
11. Rehe K, Wilson K, Bomken S, et al. Acute B lymphoblastic leukaemia-propagating cells are present at high frequency in diverse lymphoblast populations. *EMBO Mol Med*. 2013;5(1):38-51.
12. Irving J, Matheson E, Minto L, et al. Ras pathway mutations are prevalent in relapsed childhood acute lymphoblastic leukemia and confer sensitivity to MEK inhibition. *Blood*. 2014;124(23):3420-3430.
13. Williams MT, Yousafzai Y, Cox C, et al. Interleukin-15 enhances cellular proliferation and upregulates CNS homing molecules in pre-B acute lymphoblastic leukemia. *Blood*. 2014;123(20):3116-3127.
14. Halsey C, Docherty M, McNeill M, et al. The GATA1s isoform is normally down-regulated during terminal haematopoietic differentiation and over-expression leads to failure to repress MYB, CCND2 and SKI during erythroid differentiation of K562 cells. *J Hematol Oncol*. 2012;5:45.
15. Bustin SA, Benes V, Garson JA, et al. The MIQE guidelines: minimum information for publication of quantitative real-time PCR experiments. *Clin Chem*. 2009;55(4):611-622.
16. McKimmie CS, Graham GJ. Astrocytes modulate the chemokine network in a pathogen-specific manner. *Biochem Biophys Res Commun*. 2010;394(4):1006-1011.
17. Bomken S, Buechler L, Rehe K, et al. Lentiviral marking of patient-derived acute lymphoblastic leukaemic cells allows in vivo tracking of disease progression. *Leukemia*. 2013;27(3):718-721.
18. Gabriel R, Eckenberg R, Paruzynski A, et al. Comprehensive genomic access to vector integration in clinical gene therapy. *Nat Med*. 2009;15(12):1431-1436.
19. Price RA. Histopathology of CNS leukemia and complications of therapy. *Am J Pediatr Hematol Oncol*. 1979;1(1):21-30.
20. Buonamici S, Trimarchi T, Ruocco MG, et al. CCR7 signalling as an essential regulator of CNS infiltration in T-cell leukaemia. *Nature*. 2009;459(7249):1000-1004.

21. Gomez AM, Martinez C, Gonzalez M, et al. Chemokines and relapses in childhood acute lymphoblastic leukemia: A role in migration and in resistance to antileukemic drugs. *Blood Cells Mol Dis*. 2015;55(3):220-227.
22. Den Boer ML, van Slegtenhorst M, De Menezes RX, et al. A subtype of childhood acute lymphoblastic leukaemia with poor treatment outcome: a genome-wide classification study. *Lancet Oncol*. 2009;10(2):125-134.
23. le Viseur C, Hotfilder M, Bomken S, et al. In childhood acute lymphoblastic leukemia, blasts at different stages of immunophenotypic maturation have stem cell properties. *Cancer Cell*. 2008;14(1):47-58.
24. Fehse B, Kustikova OS, Bubenheim M, Baum C. Pois(s)on--it's a question of dose. *Gene Ther*. 2004;11(11):879-881.
25. Rongvaux A, Takizawa H, Strowig T, et al. Human hemato-lymphoid system mice: current use and future potential for medicine. *Annu Rev Immunol*. 2013;31:635-674.
26. Kamel-Reid S, Letarte M, Doedens M, et al. Bone marrow from children in relapse with pre-B acute lymphoblastic leukemia proliferates and disseminates rapidly in scid mice. *Blood*. 1991;78(11):2973-2981.
27. Meyer LH, Eckhoff SM, Queudeville M, et al. Early relapse in ALL is identified by time to leukemia in NOD/SCID mice and is characterized by a gene signature involving survival pathways. *Cancer Cell*. 2011;19(2):206-217.
28. Uckun FM, Sather H, Reaman G, et al. Leukemic cell growth in SCID mice as a predictor of relapse in high-risk B-lineage acute lymphoblastic leukemia. *Blood*. 1995;85(4):873-878.
29. Ransohoff RM, Kivisakk P, Kidd G. Three or more routes for leukocyte migration into the central nervous system. *Nat Rev Immunol*. 2003;3(7):569-581.
30. Louveau A, Smirnov I, Keyes TJ, et al. Structural and functional features of central nervous system lymphatic vessels. *Nature*. 2015;523(7560):337-341.
31. Wu S, Gessner R, Taube T, et al. Chemokine IL-8 and chemokine receptor CXCR3 and CXCR4 gene expression in childhood acute lymphoblastic leukemia at first relapse. *J Pediatr Hematol Oncol*. 2006;28(4):216-220.
32. Durig J, Schmucker U, Duhrsen U. Differential expression of chemokine receptors in B cell malignancies. *Leukemia*. 2001;15(5):752-756.
33. Corcione A, Arduino N, Ferretti E, et al. Chemokine receptor expression and function in childhood acute lymphoblastic leukemia of B-lineage. *Leuk Res*. 2006;30(4):365-372.
34. Meyer LH, Debatin KM. Diversity of human leukemia xenograft mouse models: implications for disease biology. *Cancer Res*. 2011;71(23):7141-7144.
35. Svenningsson A, Andersen O, Edsbagge M, Stemme S. Lymphocyte phenotype and subset distribution in normal cerebrospinal fluid. *J Neuroimmunol*. 1995;63(1):39-46.
36. Cario G, Izraeli S, Teichert A, et al. High interleukin-15 expression characterizes childhood acute lymphoblastic leukemia with involvement of the CNS. *J Clin Oncol*. 2007;25(30):4813-4820.
37. Krause S, Pfeiffer C, Strube S, et al. Mer tyrosine kinase promotes the survival of t(1;19)-positive acute lymphoblastic leukemia (ALL) in the central nervous system (CNS). *Blood*. 2015;125(5):820-830.
38. Holland M, Castro FV, Alexander S, et al. RAC2, AEP, and ICAM1 expression are associated with CNS disease in a mouse model of pre-B childhood acute lymphoblastic leukemia. *Blood*. 2011;118(3):638-649.

39. van der Velden VHJ, de Launaij D, de Vries JF, et al. New cellular markers at diagnosis are associated with isolated central nervous system relapse in paediatric B-cell precursor acute lymphoblastic leukaemia. *British Journal of Haematology*. 2015. doi:10.1111/bjh.13887
40. Akers SM, Rellick SL, Fortney JE, Gibson LF. Cellular elements of the subarachnoid space promote ALL survival during chemotherapy. *Leuk Res*. 2011;35(6):705-711.
41. Frishman-Levy L, Shemesh A, Bar-Sinai A, et al. Central nervous system acute lymphoblastic leukemia: role of natural killer cells. *Blood*. 2015;125(22):3420-3431.

TABLES

Table 1: Frequency of CNS engraftment in primary patient samples. Samples are grouped by cytogenetics. CNS engraftment was determined histologically and analysed blinded to patient details. TLP = Traumatic Lumbar Puncture with visible leukaemic blasts (+), without visible blasts (-).

Table 2: Clinical risk factors for CNS engraftment.

Clinical characteristics of patients whose samples infiltrated the CNS (CNS+) in the xenograft model, compared to those with no evidence of infiltration (CNS-). Cytogenetic high-risk group was defined according to the UKALL 2011 trial protocol.

FIGURE LEGENDS

Figure 1: Schematic representation of proposed mechanisms underlying CNS infiltration and subsequent relapse. In model 1 only some leukaemic cells acquire the ability to enter the CNS and the risk of CNS relapse depends on the presence or absence of a clone (shown in green) with the capacity to leave the bone marrow and enter the CNS. Different leukaemia subtypes may vary in this capacity with some (shown in blue) unable to enter the CNS compartment, others avidly traffic to the CNS (shown in

green), whilst some acquire this capacity in rare subclones (mixed purple, blue and green). In model 2 all leukaemic cells may have the ability to seed this compartment and sub-clinical CNS involvement at diagnosis may be universal and show little or no subclonal selection (model 2). In both cases, CNS relapse may also be determined by whether cells can adapt to the foreign microenvironment of the CNS and evade elimination by ALL-directed therapy and/or immunological surveillance (in this example green and/or yellow subclones have been selected for at relapse).

Figure 2: Histological analysis of brains from xenografted mice. (a) Line drawing of a coronal section of murine brain showing approximate locations (zones) of images shown in (b)-(d). **(b)** Photomicrographs of H&E stained brain sections. Top image: low-power view of cerebral cortex and leptomeninges (x5), bottom image: close-up of a central meningeal vessel (x40). Long thin arrow indicates leukaemic cells in the vessel wall. Black scale bar = 100μm **(c)** H&E (top row), and corresponding anti-human CD45 (bottom row), staining of leukaemic deposits. Left-hand panel: cells surrounding the dural venous sinus (x20). Central panel: cells within choroid-plexus (x20). Right-hand panel: high-power view of meninges (x40). Black bar = 100μm **(d)** post-mortem image of grade 2 arachnoid leukaemia (zone ii) in a child with ALL – H&E (x33) – reproduced with permission from Price and Johnson [4] **(e)** H&E of representative coronal sections (all zone iv) from mice engrafted with a CNS-3 sample and 5 matched CNS-1 controls (x40). Black bar = 50μm.

In all images: thick black arrows mark the leukaemic infiltrate within the leptomeninges and black stars (*****) mark leukaemic infiltrates within the calvarial bone marrow cavity. # denotes the sample identifier in Table 1.

Figure 3: Chemokine receptors and CNS engraftment. (a) Flow cytometry for chemokine receptor expression in BCP-ALL. Isotype control - shaded histogram, specific staining - open histogram. Samples names and associated translocations shown, CNS+ indicates the results of xenografting this sample into mice with Y= evidence of CNS engraftment and N= no evidence of CNS engraftment **(b)** Quantitative PCR for chemokine ligand expression by cultured human primary meningeal cells (white bars) and choroid plexus epithelial cells (black bars) (both passage 3). Arbitrary expression values were derived from ΔCT. **(c)** Primary ALL cells from 1 CNS-3 patient (open symbols) and 4 CNS-1 matched controls (closed symbols) were retrieved from BM and meninges of xenografted mice and analysed by flow cytometry. Contaminating murine cells were excluded by gating on human CD45. 10^5 events were analysed where possible. Data represent adjusted mean fluorescence intensity ($MFI_{specific}$ - $MFI_{isotype}$) of live leukaemic cells (huCD45+/Draq7-). Bars represent means of adjusted MFIs. Differences between CNS and BM expression were analysed using two-tailed paired student t-tests. (d) Leukaemic infiltration in NSG mice engrafted with REH-luciferase-GFP expressing cells and treated with the CXCR4 inhibitor AMD3100 or PBS control. Left hand panel shows leukaemic engraftment in the bone marrow as measured by numbers of GFP-positive cells (REH-luciferase GFP) on flow cytometry. Data show mean ± SEM in n=7 and n=6 mice for PBS and AMD3100 groups respectively, analysed by an unpaired student t-test, ***$p<0.001$.Central panel shows liver infiltration quantified by counting human-$CD45^+$ cells (brown DAB-stained cells) in 8 random fields of view per section. Data show mean ± SEM for n=4 and n=5 mice in PBS and AMD3100 groups respectively, analysed by an unpaired student t-test, **$p<0.01$. Right hand panel shows histological analysis of murine brains from xenografts (n=5 mice in each group). Each brain was divided into 5 segments and sections were cut from each

segment, the maximal depth of meningeal infiltrates was recorded for each section using Axiovision Rel 4.3 software (Carl Zeiss). Data show mean ± SEM. Representative histology and IVIS imaging from these mice along with full experimental details are provided in Supplementary Figure 3.

Figure 4: CNS engraftment of sorted sub-populations of leukaemic blasts. Sorted and unsorted leukaemic blasts from 6 primografts (#4540, #M120, #WB51, #HV101, #737c and #758b), were injected intrafemorally, at limiting dilutions into the femurs of 1-4 mice each. CNS involvement was assessed histologically following transplantation of; **(a)** 10-1500 cells, or **(b)** different immunophenotypic sub-populations of leukaemic blasts. Black bars represent the number of mice in each experimental group with evidence of CNS involvement (CNS+) on histology. White bars represent number of mice without any visible CNS infiltration (CNS-). Individual results of mice injected with each cell number/immunophenotypic subpopulation for the different primografts are given in Supplementary Table 3.

Figure 5: Subclonal composition of CNS and splenic compartments. (a) Schematic of experimental design. **(b)** Clonal composition of CNS (leptomeninges) and splenic compartments of mice transplanted with primograft samples #WB51 and #L707. Pie charts show frequencies of most prevalent integrations in paired CNS and spleen samples from two mice per sample. Pie chart colours are unique to each mouse spleen-meninges pair and do not represent the same clones between different mice. Corresponding tables of integration site frequencies for each mouse are given in Supplementary Figure 5.

Table 1

Cytogenetic sub-group	Sample ID	Patients CNS status at diagnosis (cytospin)	No of mice with CNS engraftment
t(12;21)	#4630	CNS-1	0/3
	#4736	CNS-1	2/2
	#5449	CNS-1	1/2
	#5094	CNS-3	3/3
	#6112	CNS-1	1/2
	#5705	CNS-1	2/2
High Hyperdiploid	#L779	CNS-1	5/5
	#5969	CNS-1	0/2
	#6294	CNS-1	0/1
t(7;9)dic(9;20)	#21819	CNS-1	1/1
t(9;22)	#4540	TLP+	2/2
	#M120	TLP-	2/2
	#WB51	CNS-1	7/7
t(9;22), del 9p	#HV101	TLP+	2/2
Bcr-abl like	#737c	CNS-1	12/13
	#758b	CNS-1	3/5
t(11q23)	#6240	CNS-3	3/3
	#5655	CNS-1	3/3
	#4861	CNS-1	0/2
t(1;19)	#L910	CNS-1	1/1
	#BH01	CNS-1	0/3
t(8;14) – non-Burkitt	#20580	CNS-1	4/5
iAmp21	#L868	CNS-1	7/7
	#L904	CNS-1	0/2
t(17;19)	#L707	CNS-1	2/2
IgH translocation	#20951	CNS-1	3/3
CRLF2 deletion	#11538	CNS-1	4/4
No result	#L897	CNS-1	4/4
	#L920	CNS-1	1/1
13 cytogenetic groups	29 patient samples	2 CNS-3, 24 CNS-1, 3 TLP,	75/94 mice and 23/29 primary samples engrafted in CNS

Table 2

Characteristic	Category	CNS +ve n=23		CNS -ve n=6		p-value*
		n	%	n	%	
Age	<10 year	17	(77)	5	(23)	0.631
	>10 years	6	(86)	1	(10)	
Sex	Male	10	(90)	1	(10)	0.228
	Female	13	(70)	5	(30)	
WCC	WCC <100	15	(80)	4	(20)	0.947
	WCC >100	8	(80)	2	(20)	
CNS status	CNS-1	18	(80)	6	(20)	0.665
	CNS-3	2	(100)	0	(0)	
	TLP+	2	(100)	0	(0)	
	TLP-	1	(100)	0	(0)	
Cytogenetic risk	Low risk	6	(67)	3	(33)	0.455
	High risk	8	(80)	2	(20)	
	Others	9	(90)	1	(10)	
Outcome	CCR**	15	(70.0)	6	(30)	0.237
	Relapse	7	(100)	0	(0)	
	TRM	1	(100)	0	(0)	

***calculated using chi-square test**

****continuous complete remission until last follow-up**

Cytogenetic low risk **t(12;21), High Hyperdiploid**

Cytogenetic high risk **t(9;22), iAMP21, t(17;19), 11q23**

Others **t(7;9)dic(9;20), t(8;14) – non-Burkitt, bcr-abl-like, IgH translocation, CRLF2 deletion, no result**

Figure 1

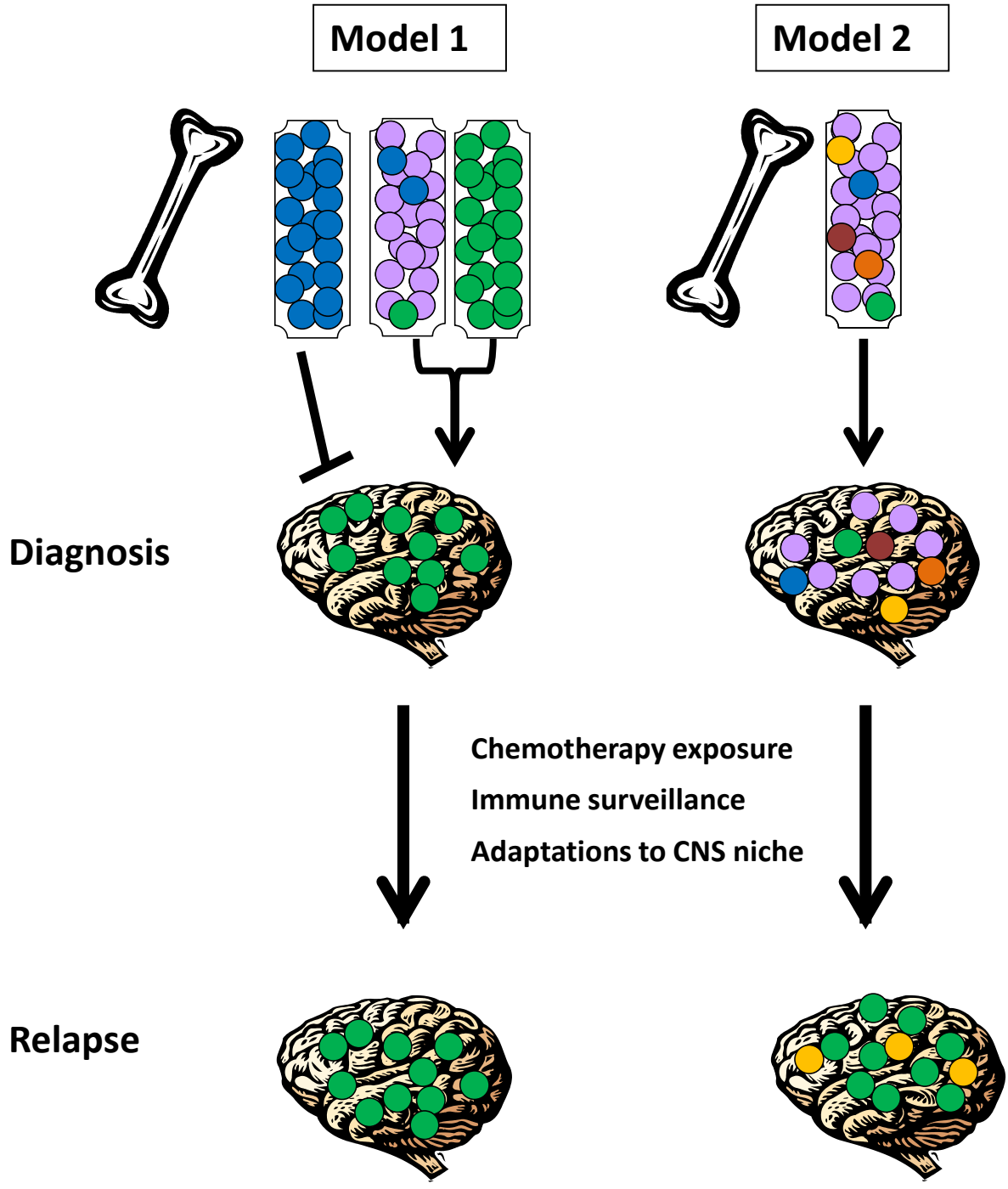
Model 1
Model 2
Diagnosis
Chemotherapy exposure
Immune surveillance
Adaptations to CNS niche
Relapse

Figure 2

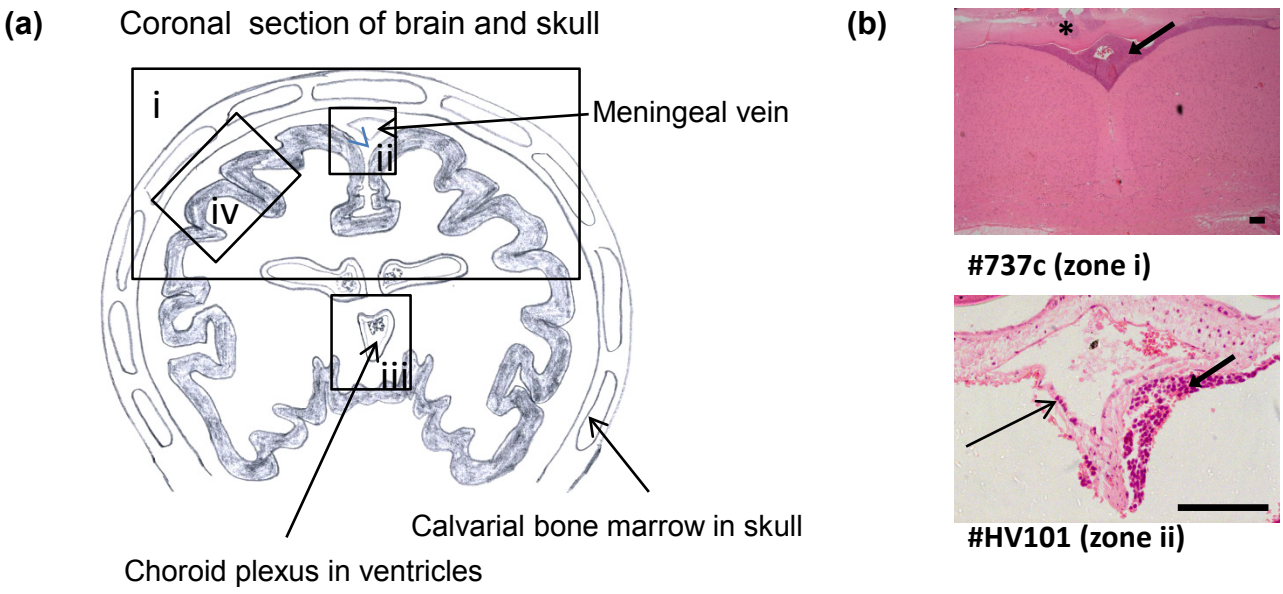
(a)
Coronal section of brain and skull
i
ii
iii
iv
Meningeal vein
Calvarial bone marrow in skull
Choroid plexus in ventricles
(b)
#737c (zone i)
#HV101 (zone ii)
(c)
#L897 (zone ii)
#L868 (zone iii)
#L868 (zone iv)
(d)
(e)
#5094 CNS-3
#4736 CNS-1
#5449 CNS-1
#6112 CNS-1
#5705 CNS-1
#4630 CNS-1

Figure 3

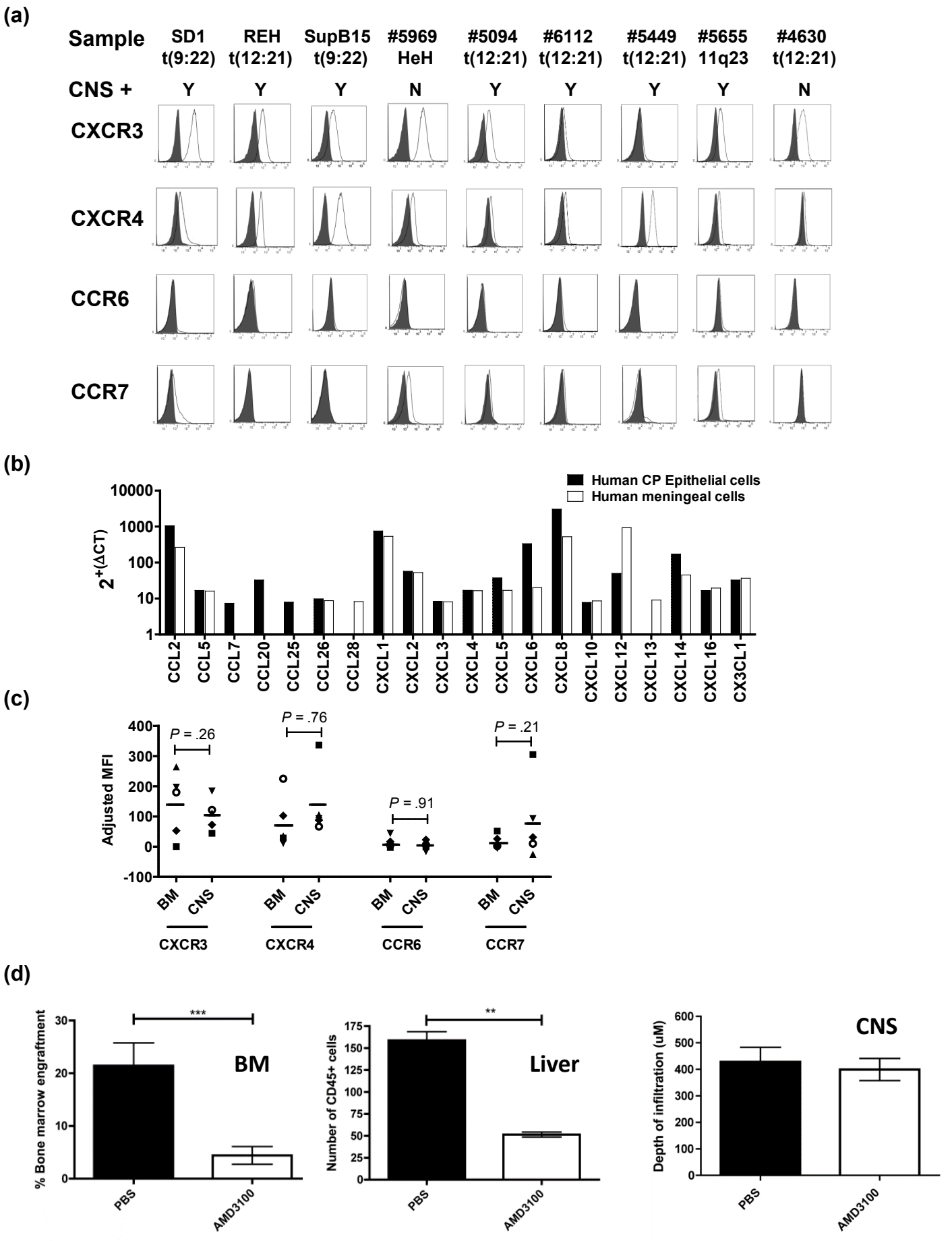
(a)
Sample
SD1 t(9:22)
REH t(12:21)
SupB15 t(9:22)
#5969 HeH
#5094 t(12:21)
#6112 t(12:21)
#5449 t(12:21)
#5655 11q23
#4630 t(12:21)
CNS +
Y Y Y N Y Y Y Y N
CXCR3
CXCR4
CCR6
CCR7
(b)
Human CP Epithelial cells
Human meningeal cells
2+(ΔCT)
10000
1000
100
10
1
CCL2 CCL5 CCL7 CCL20 CCL25 CCL26 CCL28 CXCL1 CXCL2 CXCL3 CXCL4 CXCL5 CXCL6 CXCL8 CXCL10 CXCL12 CXCL13 CXCL14 CXCL16 CX3CL1
(c)
Adjusted MFI
400
300
200
100
0
-100
P = .26
P = .76
P = .91
P = .21
BM CNS BM CNS BM CNS BM CNS
CXCR3 CXCR4 CCR6 CCR7
(d)
% Bone marrow engraftment
***
BM
PBS AMD3100
Number of CD45+ cells
**
Liver
PBS AMD3100
Depth of infiltration (uM)
CNS
PBS AMD3100

Figure 4

(a)

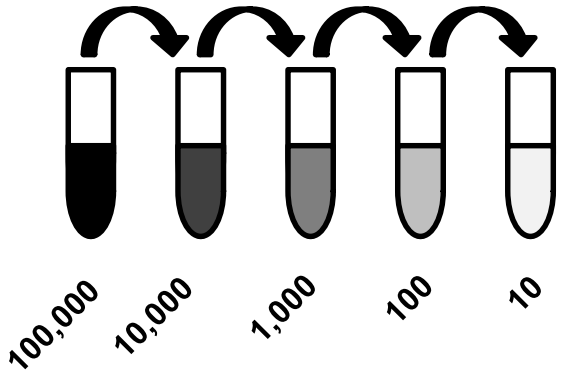
100,000
10,000
1,000
100
10

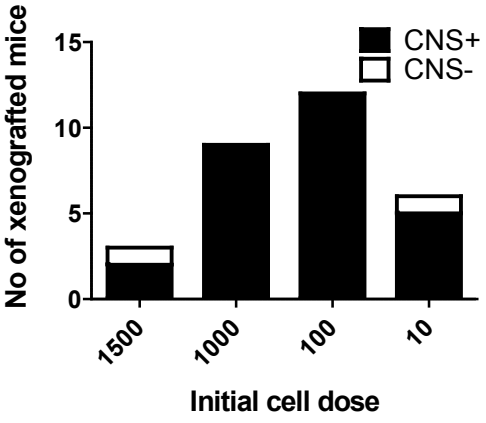
No of xenografted mice
15
10
5
0
CNS+
CNS-
1500
1000
100
10
Initial cell dose

(b)

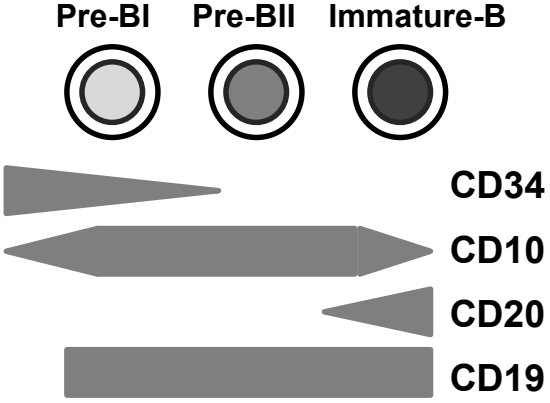
Pre-BI
Pre-BII
Immature-B
CD34
CD10
CD20
CD19

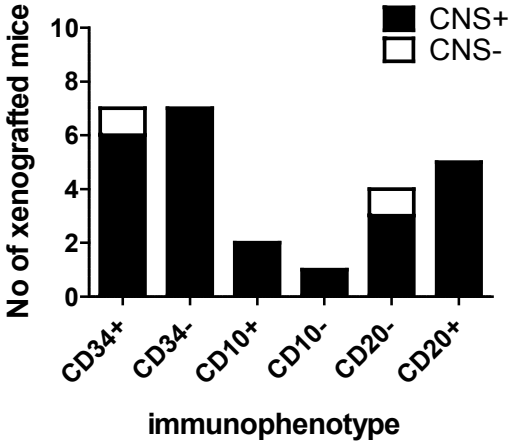
No of xenografted mice
10
8
6
4
2
0
CNS+
CNS-
CD34+
CD34-
CD10+
CD10-
CD20-
CD20+
immunophenotype

Figure 5

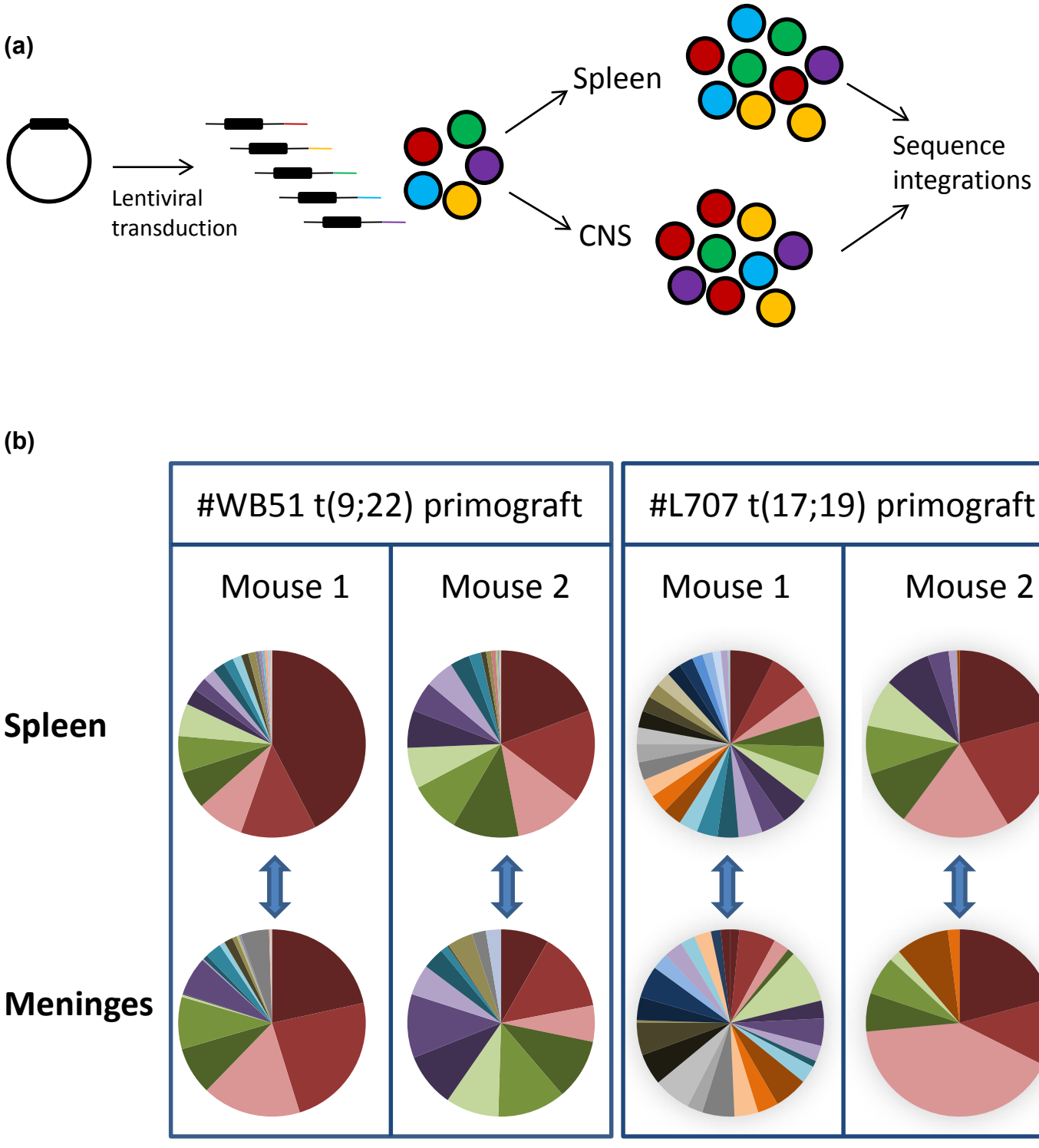
(a)
Lentiviral transduction
Spleen
CNS
Sequence integrations
(b)
#WB51 t(9;22) primograft
#L707 t(17;19) primograft
Mouse 1
Mouse 2
Mouse 1
Mouse 2
Spleen
Meninges